

Atmospheric Photooxidation Diminishes Light Absorption by Primary Brown Carbon Aerosol from Biomass Burning

Benjamin J. Sumlin,[†] Apoorva Pandey,[†] Michael J. Walker,[†] Robert S. Pattison,[‡] Brent J. Williams,[†] and Rajan K. Chakrabarty^{*,†,§}

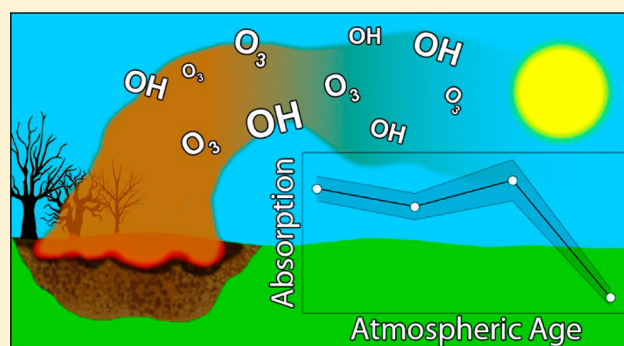
[†]Center for Aerosol Science and Engineering, Department of Energy, Environmental and Chemical Engineering, Washington University in St. Louis, St. Louis, Missouri 63130, United States

[‡]Pacific Northwest Research Station, United States Forest Service, Anchorage, Alaska 99501, United States

[§]McDonnell Center for the Space Sciences, Washington University in St. Louis, St. Louis, Missouri 63130, United States

S Supporting Information

ABSTRACT: Light-absorbing organic aerosols, optically defined as brown carbon (BrC), have been shown to strongly absorb short visible solar wavelengths and significantly impact Earth's radiative energy balance. There currently exists a knowledge gap regarding the potential impacts of atmospheric processing on the absorptivity of such particles generated from biomass burning. Climate models and satellite retrieval algorithms parametrize the optical properties of BrC aerosols emitted from biomass burning events as unchanging throughout their atmospheric lifecycle. Here, using contact-free optical probing techniques, we investigate the effects of multiple-day photochemical oxidation on the spectral (375–532 nm) optical properties of primary BrC aerosols emitted from smoldering combustion of boreal peatlands. We find the largest effects of oxidation in the near-UV wavelengths, with the 375 nm imaginary refractive index and absorption coefficients of BrC particles decreasing by ~36% and 46%, respectively, and an increase in their single scattering albedo from 0.85 to 0.90. Based on simultaneous chemical characterization of particles, we infer a transition from functionalization to fragmentation reactions with increasing photooxidation. Simple radiative forcing efficiency calculations show the effects of aging on atmospheric warming attributed to BrC aerosols, which could be significant over snow and other reflective surfaces.



INTRODUCTION

On a global scale, organic aerosols (OA) constitute a large fraction (20–90%) of the tropospheric submicron particulate matter burden.^{1,2} The optical properties of these particles are often parametrized by their effective complex refractive indices ($m = n + ik$), and in climate models, the real component n is assumed to dominate OA optical behavior, driving atmospheric cooling associated with OA negative direct radiative forcing (DRF). The positive DRF (warming effects) of light-absorbing black carbon (BC) aerosols helps offset negative DRF from OA scattering. In recent years, there has been mounting observational evidence of light-absorbing OA, optically defined as brown carbon (BrC), prevalent in substantial amounts in the atmosphere that could offset the magnitude of OA's negative DRF.^{3,4} Constraining the light absorption properties of BrC aerosols for inclusion in models poses a significant challenge for the atmospheric climate change community. BrC aerosols have a nonzero imaginary part k of its refractive index that increases toward shorter visible and ultraviolet (UV) wavelengths, resulting in an absorption Ångström exponent much larger than one.^{5,6} Variability in k values for BrC aerosols is large;

studies have suggested that in addition to the different BrC emission sources, atmospheric processes such as photooxidation, photobleaching, and volatilization could be playing major roles in explaining this large variability.^{3,7}

The low-temperature, flameless smoldering phase of biomass burning (BB) is a dominant emission source of primary BrC,^{6,8} and this aerosol constitutes up to two-thirds of the global primary OA budget.^{9–11} The chemical composition of primary BrC is complex and dependent on the fuel type and smoldering temperature. Previous BrC-related studies have focused on characterizing the optical properties of fresh aerosol emissions from BB,³ humic-like substances (HULIS), and secondary aerosol produced by photooxidation of organic precursors. Only a few recent studies have partially investigated the effects of atmospheric processing, i.e., photobleaching^{12–14} and volatilization,⁷ on the bulk absorption characteristics of BrC

Received: September 3, 2017

Revised: September 19, 2017

Accepted: September 21, 2017

Published: September 21, 2017

particles, while others focused on atmospheric processing of flaming and mixed-phase combustion.¹⁵ The influence that atmospheric transport and processing could exert on key BrC optical properties—single scattering albedo (SSA) and k —necessary for investigating the DRF life-cycle of these particles in climate models remain poorly understood. In the simplest form, atmospheric processing involves oxidation by ozone (O₃) and the hydroxyl radical (OH) in the presence of UV light. In this letter, we attempt to address this understudied phenomenon by subjecting primary BrC to accelerated oxidation. We report our findings on the effects of photochemical aging up to 4.5 equiv atmospheric days on the spectrally resolved optical properties of primary BrC aerosols generated from laboratory-scale BB.

■ EXPERIMENTAL METHODS

The biomass fuel used to generate BrC aerosols was peat collected during 2016 from an interior boreal forest near Tok, Alaska (63.32° N, 143.02° W), a region dominated by black spruce (*Picea mariana*). Notably, smoldering of peatlands has been ongoing year-round in this collection site. Smoldering forest fires in the Boreal region have been shown to be the largest contributor to OA emissions, contributing between 46% and 72% of all carbon emissions in a given year.¹⁶ Chakrabarty et al. have shown that smoldering Alaskan and Siberian peat emissions contain BrC aerosols with no BC component.⁸ It is noteworthy to mention that these BrC aerosols are distinct from “tar-ball” particles that form from pyrolysis products of BB and involve a rapid thermal transformation process upon passing through a high-temperature flaming combustion zone.^{17,18}

We conducted several controlled burn experiments, each with 30–50 g samples of dried Alaskan peat (<5% moisture content), on a computer-controlled heating plate in a 21 m³ combustion chamber. Emitted smoke was left to homogeneously mix in the sealed chamber for an hour, after which the particles were sampled continuously using a suite of instruments, namely, integrated photoacoustic-nephelometer (IPN) spectrometers,^{19,20} TSI scanning mobility particle sizer (SMPS; TSI model 3082), potential aerosol mass (PAM; Aerodyne model 001) reactor,^{21,22} and an Aerodyne high-resolution time-of-flight aerosol mass spectrometer (HR-ToF-AMS; AMS hereafter).^{23,24} A diffusion dryer removed excess water from the sample stream and a PM₁ cyclone removed all particles larger than 1 μm. The experimental setup is described in detail in the [Supporting Information](#) and summarized in [Figure S1](#).

Three IPN spectrometers, operating at 375, 405, and 532 nm, were used to measure in situ real-time light absorption and scattering coefficients (β_{abs} and β_{sca}). All optical measurements were averaged over 5 min intervals and used with time-correlated number size distribution measurements of the SMPS to determine the complex index of refraction of the particles using Lorenz-Mie (LM) theory.²⁵ All reported average values (± 1 standard deviation) were determined from these aggregate measurements and verified with repeat burns.

Four sets of experiments were conducted with the PAM reactor used at different OH concentrations to mimic a range of heterogeneous atmospheric oxidation time scales for primary BrC particles up to several days ([Table S1](#)). In recent years, these reactors have found extensive use to artificially age particles by subjecting them to high concentrations of atmospheric oxidants and strong UV light.²¹ Aging time in the PAM is determined from an offline calibration method that

relates oxidant exposure (OH_{exp}, molecules cm⁻³ s) to an equivalent real-atmosphere oxidant exposure.²⁶ During oxidation experiments involving BB emissions, competing reactions with volatile organic compounds (VOCs) could potentially deplete OH concentrations by converting OH to HO₂.^{22,27,28} We made every attempt in our study to remove VOCs using parallel-plate denuders connected to the inlet of the PAM reactor. However, there were no direct gas-phase measurements available to measure the removal efficiency of VOCs or to examine any particle-to-gas partitioning in the PAM. The best proof of our efforts is the size distribution data ([Figure S2](#)) from our burns which showed no nucleation mode that would indicate the presence of gas-phase VOCs oxidizing in the PAM and forming secondary organic aerosol (SOA). Therefore, our calculations neglect any interferences that could occur between OH and VOCs in the PAM, and our study focuses solely on the oxidation of primary BrC particles. We use the term “PAM-equivalent days” (PED) to relate the theoretical maximum OH_{exp} to real-world atmospheric oxidation time scales.

Peng et al. modeled non-OH chemistry in PAM reactors to evaluate experimental parameters that can be considered atmospherically relevant.²⁹ For this study, we used parameters that would predominantly result in aging by oxidation rather than by photolysis, which would be irrelevant in the troposphere. The ratio of F254/OH_{exp}, where F254 is the exposure to 254 nm photons, dictates the fractional dependence on photolysis reactions. In our experiments, we obtained F254/OH_{exp} values of 0, 4.26 × 10³, 1.49 × 10⁴, and 2.30 × 10⁴ cm s⁻¹ corresponding to 0, 1, 3.5, and 4.5 PED, respectively. Per Peng et al., these values imply that photolysis is only responsible for approximately 7% of aging at 4.5 PED, and oxidation chemistry is the dominant mechanism of aging (additional information may be found in the [SI](#)).

Aerosol chemical composition was measured using the AMS section of a thermal desorption aerosol gas chromatograph–aerosol mass spectrometer.³⁰ From this chemical composition data, we calculated the hydrogen–carbon (H:C) and oxygen–carbon (O:C) molar ratios, two quantities that have been used to parametrize bulk aerosol composition.³¹ As in previous experiments involving BB emissions,²⁸ a collection efficiency of 1 was assumed due to the high fraction of OA constituting submicron aerosol; high resolution analysis was used to generate elemental composition data.³²

The spherical and homogeneous composition of BrC particles from peat fires^{6,8} ([Figure S2](#)) justified the use of LM theory to retrieve their refractive indices. A computer script written in Python 3 and based on Borhen and Huffman’s²⁵ treatment of LM theory was used for inverting experimental measurements of scattering and absorption coefficients to derive the effective refractive indices. The inversion method is similar to that used by Guyon et al.³³ ([Supporting Information](#)).

■ RESULTS AND DISCUSSION

[Figure 1](#) demonstrates the decrease in near-UV BrC light absorption upon atmospheric aging, indicated by a decrease in the imaginary refractive index k and complemented by an increase in SSA, the ratio of scattering to total extinction. At 532 nm, k remains nearly constant within measurement uncertainty across the aging range, while at 375 nm, k decreases from 0.029 ± 0.001 to 0.019 ± 0.001. At 375 nm, SSA increased from 0.852 ± 0.005 to 0.898 ± 0.005, while at

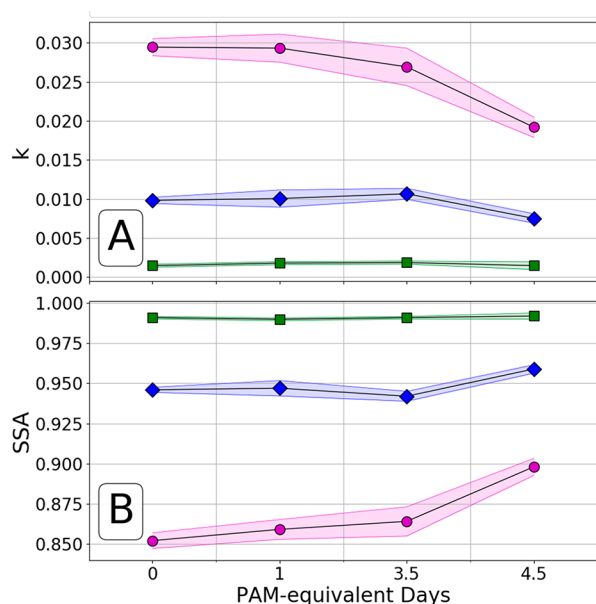


Figure 1. (A) The imaginary part k of the index of refraction decreases in the UV as particles age, indicating that the particles are losing their ability to absorb at shorter wavelengths. (B) Single scattering albedo (SSA), the ratio of scattering to total extinction, is shown to be nearly constant within error bars until later stages of aging. Error bars indicate ± 1 standard deviation.

405 nm, change in SSA upon maximum aging was ~ 0.013 . At 532 nm, the change in SSA with aging was ~ 0.001 (Table S3).

Figure 2 places our findings on k in the context of past findings involving BrC aerosol production from BB, HULIS, and secondary organic material (SOM) produced by photooxidation of organic precursors.³ Values for k found in this study are comparable with those previously reported for BB aerosols^{6,34} and HULIS.³⁵ However, the trends observed in the wavelength-dependence of k follow those of anthropogenic and biogenic SOM produced from the photooxidation of toluene, α -pinene, and limonene, as well as fulvic acid. Not shown in this figure are 405 nm refractive indices from Lambe et al.³⁶ for SOA generated from naphthalene, guaiacol, JP-10, and α -pinene as a function of O:C ratios. They reported that k increased from 1.9×10^{-4} to 3.6×10^{-3} corresponding to an increase in O:C from 0.4 to 1.3. Contrary to their findings, we find k values of primary BrC particles to decrease from 9.8×10^{-3} to 7.5×10^{-3} at 405 nm corresponding to an increase in O:C from 0.34 ± 0.01 (fresh emissions) to 0.40 ± 0.01 (4.5 PED). Hearn et al.³⁷ noted differences in reaction pathways and products from various oxidation processes from gas-phase versus condensed phase reactions which may in part explain differences observed in this study compared to the homogeneous precursor oxidation study of Lambe et al. Aging studies of primary BrC beyond O:C of 0.4 are needed to better compare these results to past studies.

The effects of oxidation processes on aerosol can be conveniently visualized with van Krevelen diagrams,³⁹ which plot H:C versus O:C ratios. These diagrams track changes in H:C and O:C ratios with photochemical processing and have been used to evaluate changes in aerosol chemical properties in both laboratory and field studies.⁴⁰ Figure 3 shows a van Krevelen diagram of the four experiments performed in this study. With increasing OH exposure, we observe that both O:C and H:C ratios increase (Table S2). The range of our measured

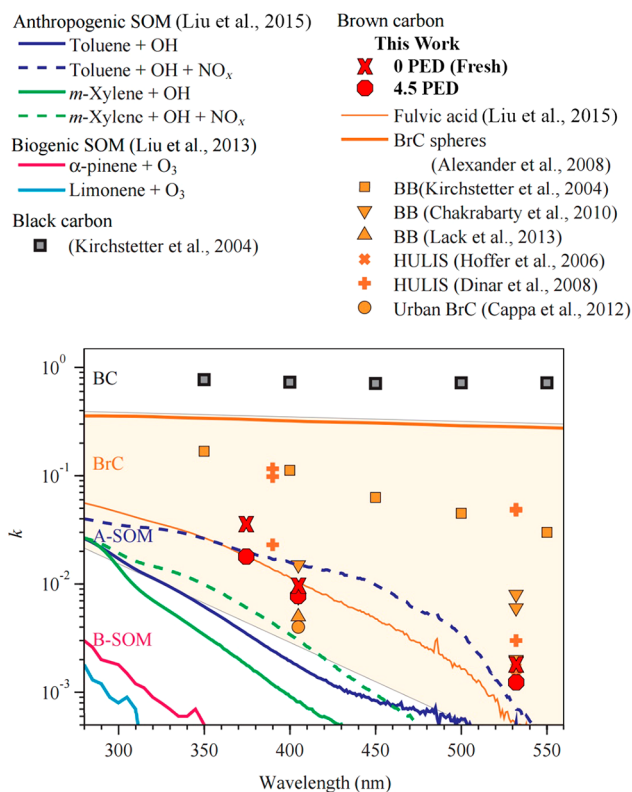


Figure 2. Comparison of the imaginary part k of the complex refractive index of fresh and aged BrC from this study with previous studies. The shaded region in the figure encompasses the range of previous observations for atmospheric BrC. The trends observed in the wavelength-dependence of primary BrC aerosol from smoldering combustion follow those of anthropogenic and biogenic secondary organic material (A-SOM and B-SOM, respectively) created from the photooxidation of various organic precursors, as well as BrC from biomass burning observed by Chakrabarty (upside-down orange triangles), Lack (orange triangles), and Cappa (orange circles). (Adapted and reprinted from Liu et al.³⁸ and available under Creative Commons Attribution License.)

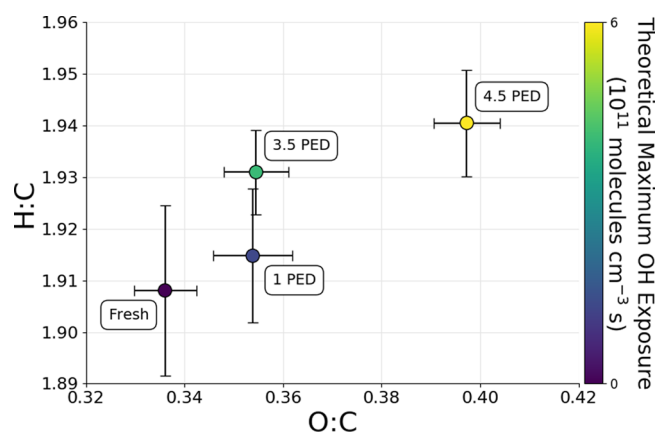


Figure 3. Van Krevelen diagram of the four experiments in this study. The color indicates the theoretical maximum OH exposure, and labels are the corresponding aging times in PED. Error bars indicate the standard deviation in the H:C and O:C measurements.

H:C are also slightly higher than those reported for oxidation of pure SOA precursors.^{41,42} Past studies have shown that, with increasing oxidation, the H:C ratio either increases⁴³ or decreases³⁶ depending on the choice of precursor and oxidant.

In our case, we attribute the increase in H:C ratio to a complex oxidation mechanism involving primary OA as a bulk material as opposed to pure precursor oxidation.^{37,44–46} The increase in O:C ratio could be attributed to the addition of oxygen-containing functional groups rather than volatilization.⁴⁷

Our results indicate a clear relationship between increasing atmospheric processing and decreasing light absorption for BrC aerosols. Chemically, this behavior could be a consequence of the transition from functionalization to fragmentation reactions with increasing photooxidation as reported by Kroll et al.³¹ and others.^{41,48,49} Fragmentation reactions reduce the size of conjugated molecular systems and could explain why BrC loses its ability to absorb light as it ages. It has been shown for squalane SOA that at O:C ratios of approximately 0.4 fragmentation completely dominates the oxidation process.⁵⁰ The O:C ratios for the BrC aerosols studied in this work were in the range of 0.34–0.4. Although functionalization-to-fragmentation transition is highly system dependent, we infer that the enhanced diminishment in aerosol light absorption between 3.5–4.5 PED could be a result of this mechanism. More detailed chemical speciation combined with simultaneous optical characterization would be required to further explore this hypothesis.

We investigated the effects of atmospheric processing on BrC aerosol light absorption reduction (Figure 4, panel A) and clear-sky DRF efficiency (panel B). The aerosol absorption

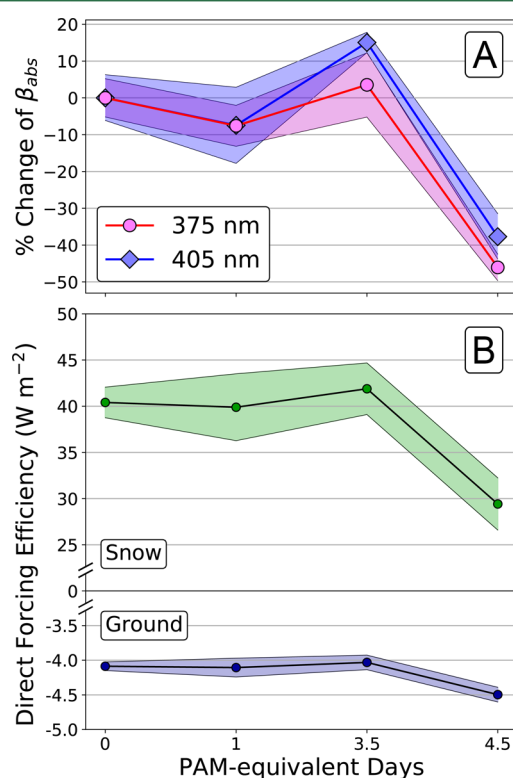


Figure 4. (A) Percent change of aerosol absorption coefficient (β_{abs}) at 375 and 405 nm. Error bars are the upper and lower bounds of Lorenz-Mie calculations using the refractive indices and their standard deviations derived in this study. (B) 375–532 nm integrated direct radiative forcing (DRF) efficiency of BrC aerosols. DRF efficiency is calculated for snow (green, positive forcing) and land (blue, negative forcing). Error bars are the upper and lower bounds of DRF efficiency calculations using average SSA ± 1 standard deviation from the experiments in this study.

coefficient (β_{abs}) depends not only on m but also on the particle number size distribution. To separate the effects of changing m and size distribution, we studied the combined effect of changing m and size distribution (Figure 4A) and two scenarios where m and size distribution were held constant (Figure S4). To isolate changing m , number geometric mean and number geometric standard deviation were held fixed at 150 nm and 1.8, respectively. In all cases, the total number concentration was held constant at $N = 10^6$ particles cm^{-3} . At 4.5 PED, the BrC β_{abs} at 375 nm decreases by $\sim 46\%$ for the combined case, $\sim 36\%$ when varying m alone, and $\sim 15\%$ when varying size distribution alone. The change in optical properties is responsible for more than twice the β_{abs} reduction than the changing size distribution alone.

The radiative forcing effect over snow (as well as other reflective surfaces such as low-level clouds) is vital to climate models, especially since this type of surface is characteristic of regions over which boreal forest fire emissions are likely to be found. BrC aerosol contributes to positive forcing (warming) over bright terrain throughout the atmospheric aging time scales investigated in this work. However, with increased atmospheric residence time from 0 to 4.5 PED, the integrated DRF efficiency decreases by approximately 27%, from 40.4 ± 1.7 to $29.4 \pm 2.8 W m^{-2}$. A corresponding decrease in DRF efficiency over ground is $\sim 5\%$, from -4.0 ± 0.0 to $-4.3 \pm 0.1 W m^{-2}$ for particle aging from fresh to 4.5 PED.

Although approximately half of the solar spectrum's energy is distributed between 400 and 700 nm, 375–532 nm forcing represents a significant warming potential over arctic terrain, providing additional momentum for climate imbalance. However, the change in optical properties at longer aging time scales imply that model-based estimates of warming due to BrC light absorption could be overestimated. Given the ubiquity of smoldering boreal peat fires, our study highlights the importance of including atmospheric processing effects of these aerosols to refine climate models and satellite retrieval algorithms. Future work needs to be conducted on investigating the effects of photooxidation on tar balls, a subset of atmospheric BrC aerosols with k values significantly higher than those investigated in this study.^{5,51}

■ ASSOCIATED CONTENT

§ Supporting Information

The Supporting Information is available free of charge on the ACS Publications website at DOI: 10.1021/acs.estlett.7b00393.

Figures and tables detailing the experimental setup; operating parameters and results; details of instrumentation used, including calibration procedures; aerosol size distributions, relative humidity, and temperature; details on computational methods for refractive index retrieval; forward Lorenz-Mie and direct radiative forcing calculations. (PDF)

■ AUTHOR INFORMATION

Corresponding Author

*Tel: +1-314-935-6054. Fax: +1-314-935-7211. E-mail: chakrabarty@wustl.edu.

ORCID

Benjamin J. Sumlin: 0000-0003-2909-7494

Michael J. Walker: 0000-0003-1347-7636

Rajan K. Chakrabarty: 0000-0001-5753-9937

Notes

The authors declare no competing financial interest.

ACKNOWLEDGMENTS

This work was partially supported by the National Science Foundation under Grant No. AGS1455215, NASA ROSES under Grant No. NNX15AI66G, and the International Center for Energy, Environment and Sustainability (InCEES) at Washington University in St. Louis. The authors thank an anonymous reviewer for insightful comments and help with improving the quality of this letter.

REFERENCES

- (1) Zhang, Q.; Jimenez, J. L.; Canagaratna, M. R.; Allan, J. D.; Coe, H.; Ulbrich, I.; Alfarra, M. R.; Takami, A.; Middlebrook, A. M.; Sun, Y. L.; et al. Ubiquity and dominance of oxygenated species in organic aerosols in anthropogenically-influenced Northern Hemisphere midlatitudes. *Geophys. Res. Lett.* **2007**, *34* (13), na.
- (2) Murphy, D. M.; Cziczo, D. J.; Froyd, K. D.; Hudson, P. K.; Matthew, B. M.; Middlebrook, A. M.; Peltier, R. E.; Sullivan, A.; Thomson, D. S.; Weber, R. J. Single-particle mass spectrometry of tropospheric aerosol particles. *J. Geophys. Res.* **2006**, *111* (D23), n/a.
- (3) Laskin, A.; Laskin, J.; Nizkorodov, S. A. Chemistry of Atmospheric Brown Carbon. *Chem. Rev.* **2015**, *115* (10), 4335–4382.
- (4) Feng, Y.; Ramanathan, V.; Kotamarthi, V. Brown carbon: a significant atmospheric absorber of solar radiation? *Atmos. Chem. Phys.* **2013**, *13* (17), 8607–8621.
- (5) Alexander, D. T. L.; Crozier, P. A.; Anderson, J. R. Brown Carbon Spheres in East Asian Outflow and Their Optical Properties. *Science* **2008**, *321* (5890), 833–836.
- (6) Chakrabarty, R.; Moosmüller, H.; Chen, L.-W.; Lewis, K.; Arnott, W.; Mazzoleni, C.; Dubey, M.; Wold, C.; Hao, W.; Kreidenweis, S. Brown carbon in tar balls from smoldering biomass combustion. *Atmos. Chem. Phys.* **2010**, *10* (13), 6363–6370.
- (7) Forrister, H.; Liu, J.; Scheuer, E.; Dibb, J.; Ziemba, L.; Thornhill, K. L.; Anderson, B.; Diskin, G.; Perring, A. E.; Schwarz, J. P.; et al. Evolution of brown carbon in wildfire plumes. *Geophys. Res. Lett.* **2015**, *42* (11), 4623–4630.
- (8) Chakrabarty, R. K.; Gyawali, M.; Yatavelli, R. L. N.; Pandey, A.; Watts, A. C.; Knue, J.; Chen, L. W. A.; Pattison, R. R.; Tsibert, A.; Samburova, V.; et al. Brown carbon aerosols from burning of boreal peatlands: microphysical properties, emission factors, and implications for direct radiative forcing. *Atmos. Chem. Phys.* **2016**, *16* (5), 3033–3040.
- (9) Bond, T. C.; Doherty, S. J.; Fahey, D.; Forster, P.; Berntsen, T.; DeAngelo, B.; Flanner, M.; Ghan, S.; Kärcher, B.; Koch, D.; et al. Bounding the role of black carbon in the climate system: A scientific assessment. *J. Geophys. Res.* **2013**, *118* (11), 5380–5552.
- (10) Bond, T. C.; Streets, D. G.; Yarber, K. F.; Nelson, S. M.; Woo, J. H.; Klimont, Z. A technology-based global inventory of black and organic carbon emissions from combustion. *J. Geophys. Res.* **2004**, *109* (D14), na.
- (11) Jacobson, M. Z. Effects of biomass burning on climate, accounting for heat and moisture fluxes, black and brown carbon, and cloud absorption effects. *J. Geophys. Res.* **2014**, *119* (14), 8980–9002.
- (12) Lee, H. J.; Aiona, P. K.; Laskin, A.; Laskin, J.; Nizkorodov, S. A. Effect of Solar Radiation on the Optical Properties and Molecular Composition of Laboratory Proxies of Atmospheric Brown Carbon. *Environ. Sci. Technol.* **2014**, *48* (17), 10217–10226.
- (13) Zhong, M.; Jang, M. Dynamic light absorption of biomass burning organic carbon photochemically aged under natural sunlight. *Atmos. Chem. Phys. Discuss.* **2013**, *13* (8), 20783–20807.
- (14) Lin, P.; Aiona, P. K.; Li, Y.; Shiraiwa, M.; Laskin, J.; Nizkorodov, S. A.; Laskin, A. Molecular Characterization of Brown Carbon in Biomass Burning Aerosol Particles. *Environ. Sci. Technol.* **2016**, *50* (21), 11815–11824.
- (15) Martinsson, J.; Eriksson, A. C.; Nielsen, I. E.; Malmberg, V. B.; Ahlberg, E.; Andersen, C.; Lindgren, R.; Nyström, R.; Nordin, E. Z.; Brune, W. H.; et al. Impacts of Combustion Conditions and Photochemical Processing on the Light Absorption of Biomass Combustion Aerosol. *Environ. Sci. Technol.* **2015**, *49* (24), 14663–14671.
- (16) Kasichke, E. S.; Hyer, E. J.; Novelli, P. C.; Bruhwiler, L. P.; French, N. H. F.; Sukhinin, A. I.; Hewson, J. H.; Stocks, B. J. Influences of boreal fire emissions on Northern Hemisphere atmospheric carbon and carbon monoxide. *Global Biogeochem. Cycles* **2005**, *19* (1), na.
- (17) Pósfai, M.; Gelencsér, A.; Simonic, R.; Arató, K.; Li, J.; Hobbs, P. V.; Buseck, P. R. Atmospheric tar balls: Particles from biomass and biofuel burning. *J. Geophys. Res.: Atmos.* **2004**, *109* (D6), n/a.
- (18) Tóth, A.; Hoffer, A.; Nyirő-Kósa, I.; Pósfai, M.; Gelencsér, A. Atmospheric tar balls: aged primary droplets from biomass burning? *Atmos. Chem. Phys.* **2014**, *14* (13), 6669–6675.
- (19) Arnott, W. P.; Moosmüller, H.; Rogers, C. F.; Jin, T.; Bruch, R. Photoacoustic spectrometer for measuring light absorption by aerosol: instrument description. *Atmos. Environ.* **1999**, *33* (17), 2845–2852.
- (20) Chakrabarty, R. K.; Moosmüller, H.; Arnott, W. P.; Garro, M. A.; Slowik, J. G.; Cross, E. S.; Han, J. H.; Davidovits, P.; Onasch, T. B.; Worsnop, D. R. Light scattering and absorption by fractal-like carbonaceous chain aggregates: Comparison of theories and experiment. *Appl. Opt.* **2007**, *46* (28), 6990–7006.
- (21) Kang, E.; Root, M. J.; Toohey, D. W.; Brune, W. H. Introducing the concept of Potential Aerosol Mass (PAM). *Atmos. Chem. Phys.* **2007**, *7*, 5727–5744.
- (22) Li, R.; Palm, B. B.; Ortega, A. M.; Hlywiak, J.; Hu, W.; Peng, Z.; Day, D. A.; Knote, C.; Brune, W. H.; de Gouw, J. A.; et al. Modeling the Radical Chemistry in an Oxidation Flow Reactor: Radical Formation and Recycling, Sensitivities, and the OH Exposure Estimation Equation. *J. Phys. Chem. A* **2015**, *119* (19), 4418–4432.
- (23) Jayne, J. T.; Worsnop, D. R.; Kolb, C. E.; Leard, D.; Davidovits, P.; Zhang, X.; Smith, K. A. Aerosol mass spectrometer for size and composition analysis of submicron particles. *J. Aerosol Sci.* **1998**, *29*, S111–S112.
- (24) DeCarlo, P. F.; Kimmel, J. R.; Trimborn, A.; Northway, M. J.; Jayne, J. T.; Aiken, A. C.; Gonin, M.; Fuhrer, K.; Horvath, T.; Docherty, K. S.; et al. Field-Deployable, High-Resolution, Time-of-Flight Aerosol Mass Spectrometer. *Anal. Chem.* **2006**, *78* (24), 8281–8289.
- (25) Bohren, C. F.; Huffman, D. R. *Absorption and Scattering of Light by Small Particles*; John Wiley & Sons, Inc., 1983.
- (26) Mao, J.; Ren, X.; Brune, W. H.; Olson, J. R.; Crawford, J. H.; Fried, A.; Huey, L. G.; Cohen, R. C.; Heikes, B.; Singh, H. B.; et al. Airborne measurement of OH reactivity during INTEX-B. *Atmos. Chem. Phys.* **2009**, *9* (1), 163–173.
- (27) Peng, Z.; Day, D. A.; Stark, H.; Li, R.; Lee-Taylor, J.; Palm, B. B.; Brune, W. H.; Jimenez, J. L. HO_x radical chemistry in oxidation flow reactors with low-pressure mercury lamps systematically examined by modeling. *Atmos. Meas. Tech.* **2015**, *8* (11), 4863–4890.
- (28) Ortega, A. M.; Day, D. A.; Cubison, M. J.; Brune, W. H.; Bon, D.; de Gouw, J. A.; Jimenez, J. L. Secondary organic aerosol formation and primary organic aerosol oxidation from biomass-burning smoke in a flow reactor during FLAME-3. *Atmos. Chem. Phys.* **2013**, *13* (22), 11551–11571.
- (29) Peng, Z.; Day, D. A.; Ortega, A. M.; Palm, B. B.; Hu, W.; Stark, H.; Li, R.; Tsigaridis, K.; Brune, W. H.; Jimenez, J. L. Non-OH chemistry in oxidation flow reactors for the study of atmospheric chemistry systematically examined by modeling. *Atmos. Chem. Phys.* **2016**, *16* (7), 4283–4305.
- (30) Williams, B. J.; Jayne, J. T.; Lambe, A. T.; Hohaus, T.; Kimmel, J. R.; Sueper, D.; Brooks, W.; Williams, L. R.; Trimborn, A. M.; Martinez, R. E.; et al. The First Combined Thermal Desorption Aerosol Gas Chromatograph—Aerosol Mass Spectrometer (TAG-AMS). *Aerosol Sci. Technol.* **2014**, *48* (4), 358–370.

- (31) Kroll, J. H.; Donahue, N. M.; Jimenez, J. L.; Kessler, S. H.; Canagaratna, M. R.; Wilson, K. R.; Altieri, K. E.; Mazzoleni, L. R.; Wozniak, A. S.; Bluhm, H.; et al. Carbon oxidation state as a metric for describing the chemistry of atmospheric organic aerosol. *Nat. Chem.* **2011**, *3* (2), 133–139.
- (32) Canagaratna, M. R.; Jimenez, J. L.; Kroll, J. H.; Chen, Q.; Kessler, S. H.; Massoli, P.; Hildebrandt Ruiz, L.; Fortner, E.; Williams, L. R.; Wilson, K. R.; et al. Elemental ratio measurements of organic compounds using aerosol mass spectrometry: characterization, improved calibration, and implications. *Atmos. Chem. Phys.* **2015**, *15* (1), 253–272.
- (33) Guyon, P.; Boucher, O.; Graham, B.; Beck, J.; Mayol-Bracero, O. L.; Roberts, G. C.; Maenhaut, W.; Artaxo, P.; Andreae, M. O. Refractive index of aerosol particles over the Amazon tropical forest during LBA-EUSTACH 1999. *J. Aerosol Sci.* **2003**, *34* (7), 883–907.
- (34) Cappa, C. D.; Che, D. L.; Kessler, S. H.; Kroll, J. H.; Wilson, K. R. Variations in organic aerosol optical and hygroscopic properties upon heterogeneous OH oxidation. *J. Geophys. Res.* **2011**, *116* (D15), na.
- (35) Dinar, E.; Abo Riziq, A.; Spindler, C.; Erlick, C.; Kiss, G.; Rudich, Y. The complex refractive index of atmospheric and model humic-like substances (HULIS) retrieved by a cavity ring down aerosol spectrometer (CRD-AS). *Faraday Discuss.* **2008**, *137*, 279–295.
- (36) Lambe, A. T.; Cappa, C. D.; Massoli, P.; Onasch, T. B.; Forestieri, S. D.; Martin, A. T.; Cummings, M. J.; Croasdale, D. R.; Brune, W. H.; Worsnop, D. R.; et al. Relationship between Oxidation Level and Optical Properties of Secondary Organic Aerosol. *Environ. Sci. Technol.* **2013**, *47* (12), 6349–6357.
- (37) Hearn, J. D.; Renbaum, L. H.; Wang, X.; Smith, G. D. Kinetics and products from reaction of Cl radicals with dioctyl sebacate (DOS) particles in O₂: a model for radical-initiated oxidation of organic aerosols. *Phys. Chem. Chem. Phys.* **2007**, *9* (34), 4803.
- (38) Liu, P. F.; Abdelmalki, N.; Hung, H. M.; Wang, Y.; Brune, W. H.; Martin, S. T. Ultraviolet and visible complex refractive indices of secondary organic material produced by photooxidation of the aromatic compounds toluene and *m*-xylene. *Atmos. Chem. Phys.* **2015**, *15* (3), 1435–1446.
- (39) van Krevelen, D. Graphical-statistical method for the study of structure and reaction processes of coal. *Fuel* **1950**, *24*, 269–284.
- (40) Heald, C. L.; Kroll, J. H.; Jimenez, J. L.; Docherty, K. S.; DeCarlo, P. F.; Aiken, A. C.; Chen, Q.; Martin, S. T.; Farmer, D. K.; Artaxo, P. A simplified description of the evolution of organic aerosol composition in the atmosphere. *Geophys. Res. Lett.* **2010**, *37* (8), na.
- (41) Lambe, A. T.; Onasch, T. B.; Croasdale, D. R.; Wright, J. P.; Martin, A. T.; Franklin, J. P.; Massoli, P.; Kroll, J. H.; Canagaratna, M. R.; Brune, W. H.; et al. Transitions from Functionalization to Fragmentation Reactions of Laboratory Secondary Organic Aerosol (SOA) Generated from the OH Oxidation of Alkane Precursors. *Environ. Sci. Technol.* **2012**, *46* (10), 5430–5437.
- (42) Nakayama, T.; Sato, K.; Matsumi, Y.; Imamura, T.; Yamazaki, A.; Uchiyama, A. Wavelength Dependence of Refractive Index of Secondary Organic Aerosols Generated during the Ozonolysis and Photooxidation of α -Pinene. *SOLA* **2012**, *8* (0), 119–123.
- (43) Kim, H.; Liu, S.; Russell, L. M.; Paulson, S. E. Dependence of Real Refractive Indices on O:C, H:C and Mass Fragments of Secondary Organic Aerosol Generated from Ozonolysis and Photooxidation of Limonene and α -Pinene. *Aerosol Sci. Technol.* **2014**, *48* (5), 498–507.
- (44) George, I. J.; Abbatt, J. P. D. Heterogeneous oxidation of atmospheric aerosol particles by gas-phase radicals. *Nat. Chem.* **2010**, *2* (9), 713–722.
- (45) Kroll, J. H.; Lim, C. Y.; Kessler, S. H.; Wilson, K. R. Heterogeneous Oxidation of Atmospheric Organic Aerosol: Kinetics of Changes to the Amount and Oxidation State of Particle-Phase Organic Carbon. *J. Phys. Chem. A* **2015**, *119* (44), 10767–10783.
- (46) Slade, J. H.; Knopf, D. A. Heterogeneous OH oxidation of biomass burning organic aerosol surrogate compounds: assessment of volatilisation products and the role of OH concentration on the reactive uptake kinetics. *Phys. Chem. Chem. Phys.* **2013**, *15* (16), 5898.
- (47) Smith, J. D.; Kroll, J. H.; Cappa, C. D.; Che, D. L.; Liu, C. L.; Ahmed, M.; Leone, S. R.; Worsnop, D. R.; Wilson, K. R. The heterogeneous reaction of hydroxyl radicals with sub-micron squalane particles: a model system for understanding the oxidative aging of ambient aerosols. *Atmos. Chem. Phys. Discuss.* **2009**, *9* (1), 3945–3981.
- (48) Ng, N. L.; Canagaratna, M. R.; Zhang, Q.; Jimenez, J. L.; Tian, J.; Ulbrich, I. M.; Kroll, J. H.; Docherty, K. S.; Chhabra, P. S.; Bahreini, R.; et al. Organic aerosol components observed in Northern Hemispheric datasets from Aerosol Mass Spectrometry. *Atmos. Chem. Phys.* **2010**, *10* (10), 4625–4641.
- (49) Daumit, K. E.; Kessler, S. H.; Kroll, J. H. Average chemical properties and potential formation pathways of highly oxidized organic aerosol. *Faraday Discuss.* **2013**, *165*, 181.
- (50) Kroll, J. H.; Smith, J. D.; Che, D. L.; Kessler, S. H.; Worsnop, D. R.; Wilson, K. R. Measurement of fragmentation and functionalization pathways in the heterogeneous oxidation of oxidized organic aerosol. *Phys. Chem. Chem. Phys.* **2009**, *11* (36), 8005.
- (51) Hoffer, A.; Tóth, A.; Nyirő-Kósa, L.; Pósfai, M.; Gelencsér, A. Light absorption properties of laboratory-generated tar ball particles. *Atmos. Chem. Phys.* **2016**, *16* (1), 239–246.